NASA Contractor Report 198226

ICASE Report No. 95-71

NASA-CR-198226
19960009105

ICASE

VISUALIZING TURBULENT MIXING OF GASES AND PARTICLES

Kwan-Liu Ma
Philip J. Smith
Sandeep Jain

NASA Contract No. NAS1-19480
October 1995

Institute for Computer Applications in Science and Engineering
NASA Langley Research Center
Hampton, VA 23681-0001

Operated by Universities Space Research Association

National Aeronautics and Space Administration

Langley Research Center
Hampton, Virginia 23681-0001

Visualizing Turbulent Mixing of Gases and Particles

Kwan-Liu Ma[†]
Institute for Computer Applications in Science and Engineering
NASA Langley Research Center
Hampton, Virginia 23681-0001

Philip J. Smith and Sandeep Jain
Department of Chemical and Fuels Engineering
University of Utah
Salt Lake City, Utah 84112

Abstract

A physical model and interactive computer graphics techniques have been developed for the visualization of the basic physical process of stochastic dispersion and mixing from steady-state CFD calculations. The mixing of massless particles and inertial particles is visualized by transforming the vector field from a traditionally Eulerian reference frame into a Lagrangian reference frame. Groups of particles are traced through the vector field for the mean path as well as their statistical dispersion about the mean position by using added scalar information about the root mean square value of the vector field and its Lagrangian time scale. In this way, clouds of particles in a turbulent environment are traced, not just mean paths. In combustion simulations of many industrial processes, good mixing is required to achieve a sufficient degree of combustion efficiency. The ability to visualize this multiphase mixing can not only help identify poor mixing but also explain the mechanism for poor mixing. The information gained from the visualization can be used to improve the overall combustion efficiency in utility boilers or propulsion devices. We have used this technique to visualize steady-state simulations of the combustion performance in several furnace designs.

[†]This research was supported in part by the National Aeronautics and Space Administration under NASA contract NAS1-19480 while the author was in residence at the Institute for Computer Applications in Science and Engineering (ICASE), NASA Langley Research Center, Hampton, VA 23681-0001.

1 Introduction

In computational studies of reactive-flow applications, such as combustion and chemical reactor design and trouble-shooting, the physical mechanisms of dispersion and mixing are often what the engineer is trying to understand. For the results of these computations, traditional visualization methods such as particle tracing, cutting planes and contour surface plots do not provide this mechanistic insight since they only display the result of mixing, they do not display the process of mixing. A *cloud tracing* technique has been developed to address visualization of these mechanisms [8]. In this paper, we extend that method to include inertial particles and to clarify the physical basis and properties of the visualization of these clouds.

The cloud visualization method is based on transforming the vector field from a traditionally Eulerian (fixed) reference frame into a Lagrangian (moving) reference frame. Mean fluid elements are traced through the computed vector field (as in traditional particle tracing methods). The statistical dispersion of the fluid elements about the mean position is also computed by using added scalar information about the root mean square value for the vector field and its Lagrangian time scale. These scalar values can usually be computed easily from existing information in computational fluid dynamics codes (i.e. turbulence models, etc.). In this way ensemble averaged "clouds of particles" are traced not just mean paths. Clouds of fluid elements and inertial particles are useful in distinguishing multi-phase mixing effects.

Each cloud follows the mean particle path and has a tube like shape, which should be distinguished from the traditional streamtubes [2] and their variants [5]. In essence, clouds differ from streamtubes in that they are derived from mean components of the velocity vector but come from fluctuating components. A cloud can cross streamlines due to eddy transport whereas a streamtube does not. A streamtube may be treated as if isolated from the adjacent fluid. As will be shown, a cloud can be viewed as the ensemble average, spatial probability distribution function of all particles starting from a given location.

The cloud visualization procedure allows a user to independently select what scalar value should be used to represent the color of the surface of a cloud. This is particularly useful in multi-phase mixing and reaction applications since the scalar properties of either phase can be used to color the cloud. The properties of the cloud are computed from ensemble average statistics of the dispersing particles due to fluid turbulence. This characteristic is discussed by Jain [7] and results in a visualization algorithm that is closer to the physical mixing process than alternate visualization schemes.

The physical model used to simulate the turbulent dispersion phenomenon is described in Section 2. Visualization results derived based the model are shown and discussed in Section 3. The three-dimensional computer graphics techniques that we have developed for this research are described in [8].

2 A 3D Turbulent Particle Dispersion Model

The dispersion of particles or fluid elements by turbulent motion has been an active field of research in recent years. Practical interests are widespread and include the combustion of particulate and droplet fuels, the pneumatic transport of particles, the mixing and settling of particles, particle deposition, electrostatic precipitation, and particle fluid separations. Practical combustion processes like spray combustion, pulverized coal and coal slurry combustion, fluidized beds, sorbent injection, and hazardous waste incineration, introduce the fuel as particles, liquid droplets, or slurries into turbulent environments.

Mixing and dispersion of gaseous streams involves fluid elements that disperse like particles but without any added inertial effects of particles with drag. The equations used here were developed by Batchelor [1]. They have been extended and used for turbulent dispersion of inertial particles in a model for the stochastic transport of particles, referred to as the STP model [3]. This approach is an efficient stochastic Lagrangian scheme that does not compromise accuracy. A 3D implementation and extension of the scheme has been described by Jain [7].

Mathematically, in the particle cloud approach, we are tracking the evolution of a probability density function (pdf) for particle position with respect to residence time. A multivariate normal pdf is used to describe the distribution of particles in the cloud. The general formula is

$$P(x_i,t) = \frac{|(\sigma_{ij})^{-1}|^{1/2}}{(2\pi)^{n/2}} e^{\frac{-1}{2g(x_i)}} \tag{1}$$

where,

$$g(x_i) = \sum_{i,j=1}^{n} (x_i - < x_i >)(x_i - < x_i >)(\sigma_{ij})^{-1} \tag{2}$$

However, there is rarely enough information about a turbulent flow field to evaluate the off diagonal terms of the variance tensor σ_{ij}. If they are assumed to be zero, the resulting pdf has the following form:

$$P(x_i,t) = \frac{1}{(8\pi)^{(3/2)} \prod_{i=1}^{3} \sigma_i} e^{-s/2} \tag{3}$$

where

$$s = s(x_i,t) = \sum_{i=1}^{3} (\frac{x_i - \mu_i}{\sigma_i})^2 \tag{4}$$

In the above equations the pdf is completely described in terms of two vectors, the mean (expected value), μ_i, and the variance (second moment), σ^2 [‡], which vary explicitly with residence time.

[‡]The notation σ_i^2 for the variance in the i direction refers to the σ_{ii} component of the variance tensor.

2.1 Mean of the Particle pdf

The mean of the pdf at some residence time, represents the most likely location of the particles in the cloud. The mean location is obtained by integrating the particle velocity which is defined by an equation of motion for the cloud particles.

$$\mu_i(t) \equiv \langle x_i(t) \rangle = \int_0^t \langle V_i(t_1) \rangle dt_1 + \langle x_i(0) \rangle \tag{5}$$

For a small heavy spherical particle the Basset-Bousineq-Oseen (BBO) equation of motion reduces to the form [9].

$$m_p \frac{d\langle V_i \rangle}{dt} = m_p \frac{3}{4} C_D \frac{\rho_f}{\rho_p} \frac{1}{d_p} (\langle U_i \rangle - \langle V_i \rangle) + (m_p - m_f) g_i \tag{6}$$

The first term on the right hand side of the equation represents the force acting on a particle due to the aerodynamic drag. The drag coefficient, is calculated using a non-linear Stokes law, in terms of the particle Reynolds number,

$$R_{e_p} = \frac{d_p |V - U| \rho_f}{\mu_f} \tag{7}$$

In the creeping flow regime the drag coefficient can be obtained by using a non-linear Stoke's law relationship

$$C_D = \frac{24}{(Re_p)} (1 + 0.15 Re_p^{0.687}) \tag{8}$$

The second term on the right hand side of Eq. 6 denotes external forces such as gravity. Additional terms in the equation of motion, describing virtual mass, thrust, Magnus, Basset, and Saffman forces, etc. have a contribution of less than 1% for the particles under consideration in various flows. Consequently, they are neglected in this analysis.

The angle brackets, $\langle\rangle$, used in the equation of motion imply ensemble average values. If N identical experiments are performed, then an ensemble average is defined as,

$$\langle V \rangle = \frac{\sum_{l=1,N} V_l}{N} \tag{9}$$

The ensemble average represents the most likely occurrence of an event with several realizations. Thus, the particle trajectory obtained, by solving an equation of motion in terms of ensemble average values, has the weighted effect of all the possible realizations of the particle(s) represented by the cloud and represents the statistical mean of the cloud. The ensemble average value can be equated mathematically to the expected value or the first moment of a positional pdf, which is the basis for the first equality in Eq. 5. An ensemble average gas velocity can be obtained as the expected value of its pdf as,

$$\langle U(x_i, t) \rangle = \int_{-\infty}^{\infty} U(x, t) P(U) dU \tag{10}$$

2.2 Variance of the Particle pdf

The other variable required for defining the cloud is the variance, σ^2 which is a measure of the spread of the pdf around the mean location in each co-ordinate direction. The variance is defined in terms of the fluctuating components. If we write the instantaneous values of velocity and position in terms of the mean and fluctuating components as,

$$v = \langle V \rangle + v' \tag{11}$$

$$x = \langle X \rangle + x' \tag{12}$$

then the variance of the pdf, by definition, is the ensemble average of the mean square displacements of the cloud particle positions. The ordinary differential equation governing its evolution with time can be derived as:

$$\frac{d\sigma_i^2}{dt} = \frac{dx'^2_i}{dt} = 2\int_0^t \langle v_i'(t) v_i'(t_1) \rangle dt_1 \tag{13}$$

This result can be expressed in terms of a classical turbulence property, namely, the particle velocity correlation function. It's basis lies in Taylor's work on the Lagrangian description of particle dispersion and is defined as [6]

$$R_{ij}^p(t, t_1) = \frac{\langle v_i'(t) v_j'(t_1) \rangle}{[\langle v_i'^2(t) \rangle \langle v_j'^2(t) \rangle]^{1/2}} \tag{14}$$

Substituting this in Eq. 13 and integrating provides a relationship for the variance in terms of two particle turbulence statistical quantities: the mean square velocity fluctuations, and the particle velocity correlation function, $R^p(\tau)$, as originally derived by Batchelor [1]:

$$\sigma_{ij}(t) = 2\int_0^t \int_0^{t_2} \langle v_i'(t_1) v_j'(t_2) \rangle dt_1 dt_2 \tag{15}$$

$$\sigma_{ij}(t) = 2\int_0^t \int_0^{t_2} [\langle v_i'^2(t_1) v_j'^2(t_2) \rangle]^{1/2} [R_{ij}^p(t_1, t_2) + R_{ji}^p(t_1, t_2)] dt_1 dt_2 \tag{16}$$

The variance tensor, σ_{ij}, thus obtained, would be used in the general form of the pdf given by Eq. 1 and Eq. 2.

2.3 The Particle Velocity Correlation Function

The particle velocity correlation as defined by Eq. 14 represents the rate at which the instantaneous velocity of the particle at some point (corresponding to residence time, t) loses its effect as we move away (to a location corresponding to time t_1). It is a measure of the time scale, T, over which a velocity fluctuation remains correlated. At $\tau = 0$ the velocity is fully correlated with

itself and its value is 1. As we move away, the particle velocity loses its correlation monotonically and drops asymptotically to 0. The particle velocity correlation, R^p, is different from the Lagrangian fluid velocity correlation, R^f. which can be defined similarly, in terms of the fluid fluctuating velocities.

The equations presented in this section have been derived by Wang [12] and further mathematical details of the derivation can be found in his dissertation.

The derivation proceeds in two main steps. First, the particle velocity correlation is related to that of a fluid element moving along the particle trajectory. The correlation function for this fluid element is then related to fluid Eulerian velocity correlations. Combining the above two relations the particle velocity correlation is found in terms of three dimensionless Eulerian turbulence parameters; the Stokes number, the drift parameter, and the turbulence structure parameter. Since the fluctuating components of the velocities are of interest here, this analysis is developed in a moving Eulerian reference frame.

Most analyses in the past have not distinguished between the particle and fluid element correlations. Reeks [11], and Pismen and Nir [10] have taken this into account. However, their complex analysis of the relation between fluid Lagrangian and Eulerian velocities has made their final results mathematically unwieldy. Wang has avoided this by using an approach similar to Csanady's [4], while including inertial effects at the same time.

The particle velocity correlation tensor

$$R^p_{ij}(\tau) = \langle v'_i(t) v'_j(t+\tau) \rangle \tag{17}$$

is related to the fluid velocity correlation tensor along the particle trajectory, namely

$$R^f_{ij}(\tau) = \langle u^p_i(0) v^p_j(t+\tau) = \langle u'_i(x(0),0) u'_j(x(\tau),\tau) \rangle \rangle \tag{18}$$

The particle equation of motion can be integrated [11] to give the particle velocity

$$v_i = \int_{-\infty}^{t} \frac{u_i(x(\tau),\tau)}{\tau_a} exp(\frac{\tau - t}{\tau_a}) d\tau + v_d \delta_{i3} \tag{19}$$

Maxey [9] has shown that the mean velocity of a particle is slightly larger than v_d (by less than 3-5% in most cases). If this difference is neglected the instantaneous fluctuating velocity of the particle can be found as

$$v'_i(t) \equiv v_i(t) - \langle v_i(t) \rangle = v_i(t) - v_d \delta_{i3} \tag{20}$$

Combining Eq. 18, Eq. 19, and Eq. 20

$$R^p_{ij}(\tau) = \frac{1}{\tau_a^2} \int_{-\infty}^{0} \int_{-\infty}^{\tau} R^f_{ij}(\tau_1 - \tau_2) exp(\frac{\tau_1 + \tau_2 - \tau}{\tau_a}) d\tau_a d\tau_2 \tag{21}$$

Partial integration of Eq. 21 gives

$$R^p_{ij}(\tau) = \frac{1}{2\tau_a} \int_{-\infty}^{\infty} exp(-\frac{|\xi - \tau|}{\tau_a}) R^f_{ij}(\xi) d\xi \tag{22}$$

This relation shows the difference between the velocity correlation for a particle and a fluid element moving along the particle trajectory, due to particle inertia. Reeks [11] has derived this same equation. It can be seen that Csanady's assumption of $R^p = R^f$ is good only if $\tau_a \rightarrow 0$, i.e., zero inertia particles.

Next, to relate $R^p_{ij}(\tau)$ to available fluid turbulence statistics, Csanady's approach [4] is used and modified to include the effects of inertia in the time scale. In this approach, the normalized velocity autocorrelations of the turbulent flow in the moving Eulerian frame are assumed to be exponential functions, namely,

$$D_L(\tau) = exp(-\frac{|\tau|}{T_L}) \tag{23}$$

$$D_{mE}(\tau) = exp(-\frac{|\tau|}{T_{mE}}) \tag{24}$$

$$f(r) = exp(-\frac{|r|}{L_f}) \tag{25}$$

$$g(f) = (1 - \frac{|r|}{2L_f})exp(-\frac{|r|}{L_f}) \tag{26}$$

D_L is the Lagrangian fluid velocity correlation and D_{mE} is the one-point Eulerian fluid velocity temporal correlation. $f(r)$ and $g(r)$ are the longitudinal and transverse fluid velocity spatial correlations, respectively. Exponential correlations have been shown to fit experimental data [6].

For the fluid velocity correlation along the particle trajectory, with time delay, t, the mean spatial displacement of the particle in this time would be $v_d t$. Hence, a spatial correlation should be included in $R^f_{ij}(\tau)$ to account for the relative displacement. In the limiting case of $v_d \rightarrow \infty$, the particle displacement is relatively large and the spatial correlation is dominant. Thus, we have $R^f_{11} = R^f_{22}(\tau) = g(v_d\tau)$ and $R^f_{33}(\tau) = f(v_d\tau)$. In the other extreme, when $v_d \rightarrow 0$, $R^f_{ij}(\tau)$ is mainly a temporal correlation. The time scale T, for this correlation is a function of the particle inertia, and is not the same as T_L.

In general, when the effects of both inertia and drift velocity are present, there should be a smooth transition of $R^f_{ij}(\tau)$ from a fluid temporal velocity correlation to a fluid spatial velocity correlation, when the drift velocity increases from 0 to ∞. This is done by using Csanady's hypothesis that $R^f_{33}(\tau)$ is constant on the ellipses

$$\frac{\tau^2}{T^2} + \frac{V_d^2\tau^2}{L_f^2} = constant \tag{27}$$

Using the velocity correlations Eq. 23 - Eq. 27, $R^f_{ij}(\tau)$ is obtained as

$$R^f_{11}(\tau) = R^f_{22}(\tau) = u^2(1 - \frac{v_d\tau}{2L_f})exp(-\frac{\tau}{T}\sqrt{1 + m_T^2\gamma^2}) \tag{28}$$

$$R_{33}^{f}(\tau) = u^2 exp(-\frac{\tau}{T}\sqrt{1+m_T^2\gamma^2}) \tag{29}$$

where g and m_T are the drift parameter and the turbulence structure parameter respectively.

$$\gamma = \frac{v_d}{u'} = \frac{\tau_a g}{u'} \tag{30}$$

$$m_T = \frac{Tu'}{L_f} \tag{31}$$

Substituting Eq. 28 or Eq. 29 into Eq. 22, the following relationship for the particle velocity correlation is obtained

$$R_{11}^{p}(\tau) = (\frac{u'^2}{\theta})exp(-\frac{\tau}{\tau_a})(St_T\sqrt{1+m_T^2\gamma^2} - 0.5m_T\gamma St_T\frac{St_T^2(1+m_T^2\gamma^2)+1}{\theta}) +$$
$$\frac{u'^2}{\theta}exp(-\frac{\tau}{T}\sqrt{1+m_T^2\gamma^2})(-1+\frac{m_T St_T^2\gamma\sqrt{1+m_T^2\gamma^2}}{\theta}+0.5m_T\gamma\frac{\tau}{T}) \tag{32}$$

$$R_{33}^{p}(\tau) = \frac{u'^2 St_T\sqrt{1+m_T^2\gamma^2}}{\theta}exp(-\frac{\tau}{\tau_a}) - \frac{u'^2}{\theta}exp(-\frac{\tau}{T}\sqrt{1+m_T^2\gamma^2}) \tag{33}$$

where, St is the Stokes number and is a measure of the particles inertia.

$$St_T = \frac{\tau_a}{T} \tag{34}$$

and

$$\theta = St_T^2(1+m_T^2\gamma^2) - 1 \tag{35}$$

The time scale T, which is physically the time scale for a fluid element traveling along the particle trajectory, is needed. It is a function of the particle inertia. In the limit that $St \gg 1$, the particle's inertia is very large, so that the particle responds very slowly to fluctuations in fluid velocity. Consequently, the particle stays at one point for a time interval of the order of T_{mE}. Thus when $St \gg 1$. On the other hand if $St \rightarrow 0$, the particle reduces to a fluid element and $T \rightarrow T_L$. In general T is a function of St and varies between T_L and T_{mE}. Wang and Stock [13] have done a numerical simulation using turbulence generated by Fourier modes and obtained the following curve fit for T as a function of the Stokes parameter.

$$\frac{T(St)}{T_{mE}} = 1 - \frac{constant}{(1+St)^{0.4(1+0.01St)}} \tag{36}$$

where, the constant$\equiv 1 - (T_L/TmE) = 0.644$, for $m = 1$.

To get the dimensionless parameters St_T and m_T, the parameters St and m based on Eulerian time scales are first calculated as,

$$St = \frac{\tau_a}{T_{mE}} \tag{37}$$

and

$$m = \frac{T_{mE}u}{L_f} \tag{38}$$

Eq. 36 gives $T(St)$. St_T and m_T are then calculated as

$$St_T = St\frac{T_{mE}}{T(St)} \tag{39}$$

and

$$m_T = m\frac{T(St)}{T_{mE}} \tag{40}$$

We calculate T_{mE} from the fixed Eulerian parameters by an approximate relation as

$$T_{mE} = T_{fE}\frac{U}{u'} \tag{41}$$

T_L is related to T_{mE} by the turbulence parameter, m.

$$T_L = G(m)T_{mE} \tag{42}$$

$$G(m) = \frac{2}{\sqrt{\pi}}\int_0^\infty \frac{exp(-y^2)}{1+\frac{m}{\pi}[\sqrt{\pi}y\ erf(y) - 1 + exp(-y^2)]}dy \tag{43}$$

$G(m)$ goes from 1 to 0 asymptotically as m increases. This trend follows our discussion earlier, wherein as the turbulence increases, the fluid element is likely to escape the eddy quicker and T_L will decrease.

The behavior of the correlation function for various Stokes and drift parameters has been studied [12] and shown to realistically describe the different effects of particle behavior. The correlations show a smooth transition between the drift velocity and inertial effects. Also, these correlations are anisotropic providing greater dispersion in the direction parallel to the drift velocity as per the continuity effect. This anisotropy can occur even if the fluid phase turbulence statistics available are isotropic (from the $k-\varepsilon$ turbulence model, for example). This effect can be important in determining the cloud position in complex mixing systems. Wang has shown parametric zones where particle dispersion is more than the fluid dispersion as has been reported in the past. These correlations incorporate a physically realistic representation of the inertial particle effects.

3 Visualization Results

We have used the design of a low emission pulverized-coal combustion boiler as a demonstrative problem to show the utility of this visualization method for mixing of gases and particles. In this slagging boiler design the pulverized-coal fuel is feed through 10 separate burners into a U-shaped furnace. Figure 1a shows a rendered image of the furnace geometry revealing the U-shaped structure of the furnace. This shape allows for the ash to be collected as a flowing slag and "tapped" at the bottom of the U. The air is staged into three separate levels of injection to help in minimizing pollutant formation. This design is being considered for the U.S. DOE Combustion 2000 program for the design of a low emissions boiler system (LEBS) for the next century. The combustion computations have been performed by one of the authors (Smith) in support of this DOE project. The design question is to determine from numerical simulations whether the air sufficiently mixes with the pulverized-coal stream or not. We have used the *cloud tracing* visualization of both the fluid (air) streams and the inertial (pulverized-coal) streams to give insight into the extent of mixing.

The images shown in Figures 1b and 1c display some aspects of flow and reaction within the boiler. These are direct volume rendered images of the CO concentration (1b) and O_2 concentration (1c) in three-dimensional space. The view is from the side of the furnace. This more traditional visualization tool gives the combustion engineer an idea about important operational variables and infers something about the mixing process that occurred to create the results shown in this image. Before it reacts, the fuel (as visualized by the CO concentration in Figure 1b) mixes with the air (as visualized by the O_2 concentration in Figure 1c) to create regions of higher temperature. However, we still do not see where the particle streams went, or where the air streams went, or how the different streams interact.

Figures 1d through 1g use the cloud dispersion visualization scheme of this paper. Figures 1d, 1e and 1f compare the mixing and dispersion of the entraining air of part of one of the pulverized-coal streams (1f) with the coal particles from the same part of the same stream (1d and 1e). Coal particle clouds of two different particle sizes (150mm in 1d and 10mm in 1e) are compared with the fluid dispersion (1f). The surface of the dispersing cloud is colored by two different scalars (temperature for 1d & 1e and O_2 concentration for 1f) in these images. The fluid (air) streams which disperse most rapidly is obvious from this visualization. The smallest particles disperse similarly to the gases but more slowly. The largest particles disperse more slowly. The inertial particles also interact with various surfaces in the furnace and are partially or totally collected or removed from the cloud. Thus the clouds also diminish in size at various locations. One location in particular is just downstream from the bottom of the U in this furnace. At this location there is a slag screen consisting of a bank of cooled tubes crossing the furnace at an angle across the full furnace. Here many of the particles that have not impacted on the slagging furnace walls are collected on the screen. Some particles penetrate this screen and continue through the furnace section.

Figures 1g through 1h use transparency with the rendered image to show the cloud dispersion

of the same clouds as shown in Figures 1f but also includes clouds initiated in air jets starting on the side of the furnace, which allows us to see the interaction of these horizontal and vertical jets. All the figures to this point have shown the cloud surface at a distance of one standard deviation from the mean location of the cloud. Figures 1g-1h use 0.34 standard deviations to emphasize the differences between the two streams. Figure 1h shows a close up view of Figure 1g. The surface in both images is colored by the scalar value of the O_2 concentration. Figure 1i shows similar views of another set of interacting clouds.

All of these cloud tracing images show the extent of mixing of air with the reacting coal particle stream. This mixing determines the efficiency of the low emission boiler concept. The properties of the cloud in this visualization method are determined from the ensemble averaged variables across the spatial distribution at each mean residence time of the cloud.

The cloud surfaces in all of these visualizations are represented as triangular meshes which can be efficiently rendered by conventional graphics hardware. The surface is colored by using cloud properties selected by the user. During a visualization session, the user can interactively pick seed positions in the data domain and see how flows starting from these positions develop and mix together in some way.

4 Conclusions

We have shown that by using cloud dispersion concepts it is possible to visualize the dispersion and mixing of both massless or fluid particles and inertial particle systems. The cloud can interact with surfaces by sticking or rebounding the particles within the cloud. The use of hardware surface rendering provides rapid feedback on mixing and dispersion processes, and is computationally efficient enough to be interactive. This visualization technique is an effective analysis tool for practical engineering problems by applying it to data sets from three-dimensional combustion simulations. Combustion involves many physical and chemical processes whose fundamentals are not yet completely understood. This technique provides an improved insight into the mechanisms controlling high-speed mixing and combustion in utility boilers or propulsion devices. It gives visualization to the mechanism of mixing not just the result of mixing. Further insight can be obtained by using volume rendering so that the cloud content can also be visualized, not just the exterior surface of the cloud.

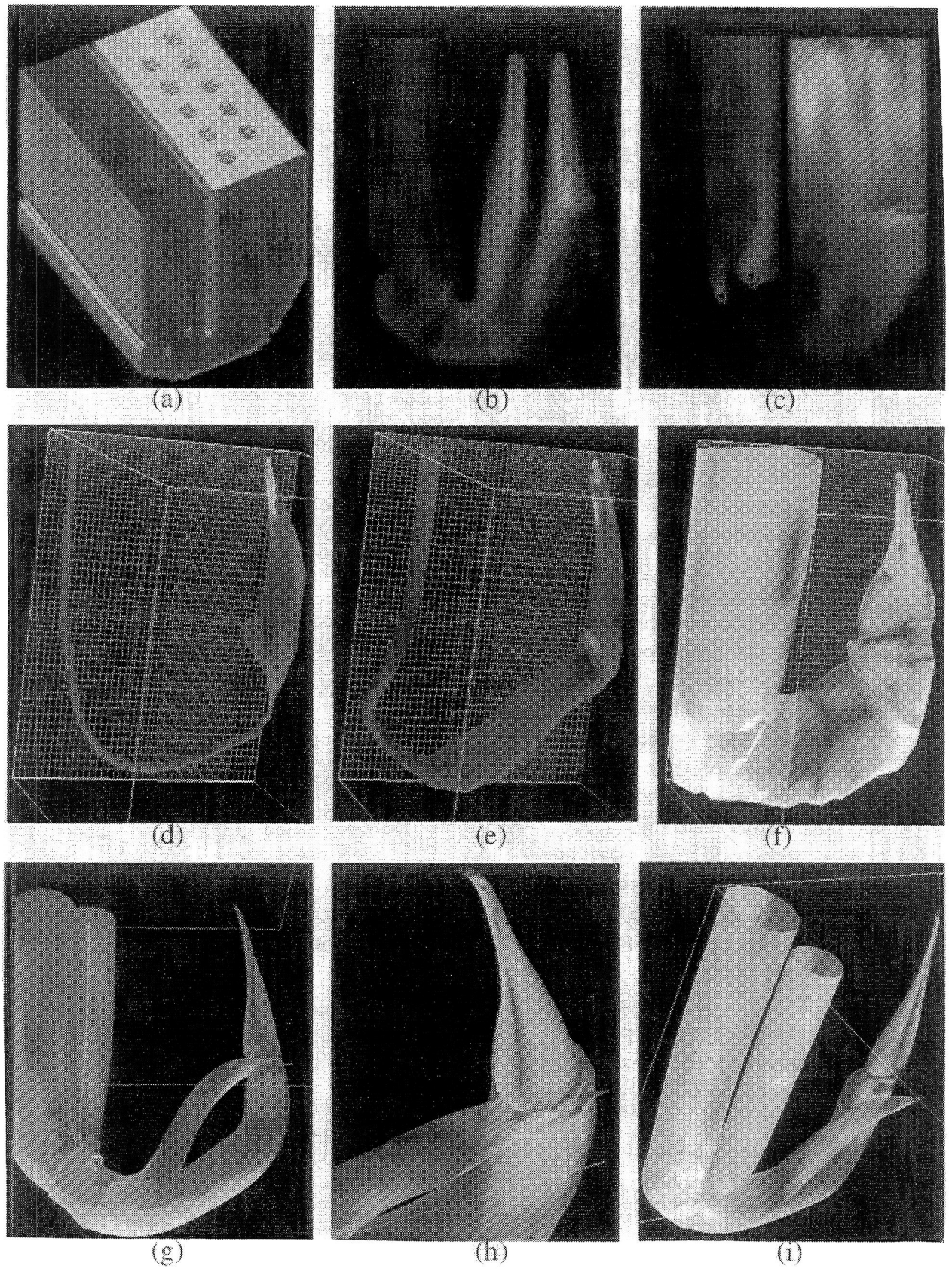

Figure 1: Visualization of Gas and Particle Mixing.

5 Nomenclature

Symbol	Units	Definition
C_D	m^{-3}	drag coefficient in the particle equation of motion
D_L		Lagrangian temporal fluid velocity correlation function
D_{mE}		One-point temporal fluid velocity correlation function
L_f	m	typical eddy length scale for fluid turbulence
m_p	kg	mass of an individual particle
m		turbulence structure parameter
n	$\frac{1}{m^3}$	average number density of particles
P	$\frac{1}{m^3}$	probability density function
R^p		particle velocity correlation function
St		Stokes number
T_g		time scale of gas turbulence
T_{fE}	s	correlation time scale in a fixed Eulerian reference frame
T_{mE}	s	correlation time scale in a moving Eulerian reference frame
T_L	s	correlation time scale in a Lagrangian reference frame
T	s	particle correlation time
t	s	residence time
t_1, t_2, τ	s	arbitrary time
u	$\frac{m}{s}$	instantaneous gas velocity
U	$\frac{m}{s}$	average gas velocity
u'	$\frac{m}{s}$	gas velocity fluctuation
v_{td}	$\frac{m}{s}$	turbulent diffusion velocity of the particle
v	$\frac{m}{s}$	instantaneous particle velocity
V	$\frac{m}{s}$	average particle velocity
v'	$\frac{m}{s}$	particle velocity fluctuation
x	m	particle location
X	m	average particle location
x'	m	fluctuation in particle position
x, y, z	m	coordinate length
β	$\frac{kg}{m^3 \cdot s}$	momentum exchange coefficient between gas and particle
γ		drift parameter
θ		constant defined by Equation 35
μ	m	mean of particle position pdf
μ_f	$\frac{kg}{m \cdot s}$	laminar viscosity of fluid phase
ρ_f	$\frac{kg}{m^3}$	density of fluid phase
ρ_p	$\frac{kg}{m^3}$	particle density
σ	m	standard deviation of pdf for particle position
δ_{ij}	-	Kronecker delta

References

[1] BATCHELOR, G. Diffusion in Free Turbulent Shear Flows. *Journal of Fluid Mechanics 67*, 3 (1957).

[2] BATCHELOR, G. K. *An Introduction to Fluid Dynamics.* Cambridge University Press, 1967.

[3] BAXTER, L., AND SMITH, P. Turbulent Dispersion of Particles. *Energy and Fuels 7* (1993), 852–859. ACS Journal.

[4] CSANADY, G. Turbulent Diffusion of Heavy Particles in the Atmosphere. *Journal of Atmos. Sci. 20* (1963).

[5] DARMOFAL, D., AND HAIMES, R. Visualization of 3-D Vector Fields: Variations on a Stream, January. 1992. AIAA Paper No. 92-0074, AIAA 30th Aerospace Science Meeting and Exhibit.

[6] HINZE, J. *Turbulence*, 2 ed. McGraw-Hill, 1975.

[7] JAIN, S. *Three-Dimensional Simulation of Turbulent Particle Dispersion Applications.* PhD thesis, Department of Chemical and Fuels Engineering, University of Utah, Salt Lake City, Utah, 1995.

[8] MA, K.-L., AND SMITH, P. J. Cloud Tracing in Convection-Diffusion Systems. In *Proceedings of Visualization'93* (October 1993), pp. 253–260.

[9] MAXEY, M. The Gravitational Settling of Aerosol Particles in Homogeneous Turbulence and Random Flow Fields. *J. Fluid Mech. 174* (1987), 441.

[10] PISMEN, L., AND NIR, A. On the Motion of Suspended Particles in STationary Homogeneous Turbulence. *Journal of Fluid Mechanics 84* (1978).

[11] REEKS, M. On the Dispersion of Small Particles Suspended in an Isotropic Turbulent Field. *Journal of Fluid Mechanics 83*, 3 (1977).

[12] WANG, L. *On the Dispersion of Heavy Particles by Turbulent Motion.* PhD thesis, Washington State University, 1990.

[13] WANG, L., AND STOCK, D. Numerical Simulation of Heavy Particle Dispersion. In *Proc. 3rd Int. Symp. Gas-Solid Flows* (1989). San Diego.

REPORT DOCUMENTATION PAGE

Form Approved
OMB No. 0704-0188

1. AGENCY USE ONLY *(Leave blank)*	2. REPORT DATE	3. REPORT TYPE AND DATES COVERED
	October 1995	Contractor Report

4. TITLE AND SUBTITLE
VISUALIZING TURBULENT MIXING OF GASES AND PARTICLES

5. FUNDING NUMBERS
C NAS1-19480
WU 505-90-52-01

6. AUTHOR(S)
Kwan-Liu Ma
Philip J. Smith
Sandeep Jain

7. PERFORMING ORGANIZATION NAME(S) AND ADDRESS(ES)
Institute for Computer Applications in Science
and Engineering
Mail Stop 132C, NASA Langley Research Center
Hampton, VA 23681-0001

8. PERFORMING ORGANIZATION REPORT NUMBER
ICASE Report No. 95-71

9. SPONSORING/MONITORING AGENCY NAME(S) AND ADDRESS(ES)
National Aeronautics and Space Administration
Langley Research Center
Hampton, VA 23681-0001

10. SPONSORING/MONITORING AGENCY REPORT NUMBER
NASA CR-198226
ICASE Report No. 95-71

11. SUPPLEMENTARY NOTES
Langley Technical Monitor: Dennis M. Bushnell
Final Report
To appear in the Proceedings of the 7th International Symposium on Flow Visualization, 1995

12a. DISTRIBUTION/AVAILABILITY STATEMENT
Unclassified–Unlimited

Subject Category 60, 61

12b. DISTRIBUTION CODE

13. ABSTRACT *(Maximum 200 words)*
A physical model and interactive computer graphics techniques have been developed for the visualization of the basic physical process of stochastic dispersion and mixing from steady-state CFD calculations. The mixing of massless particles and inertial particles is visualized by transforming the vector field from a traditionally Eulerian reference frame into a Lagrangian reference frame. Groups of particles are traced through the vector field for the mean path as well as their statistical dispersion about the mean position by using added scalar information about the root mean square value of the vector field and its Lagrangian time scale. In this way, clouds of particles in a turbulent environment are traced, not just mean paths. In combustion simulations of many industrial processes, good mixing is required to achieve a sufficient degree of combustion efficiency. The ability to visualize this multiphase mixing can not only help identify poor mixing but also explain the mechanism for poor mixing. The information gained from the visualization can be used to improve the overall combustion efficiency in utility boilers or propulsion devices. We have used this technique to visualize steady-state simulations of the combustion performance in several furnace designs.

14. SUBJECT TERMS
Computational Fluid Dynamics; Combustion; Scientific Visualization;
Multiphase Mixing

15. NUMBER OF PAGES
15

16. PRICE CODE
A03

17. SECURITY CLASSIFICATION OF REPORT	18. SECURITY CLASSIFICATION OF THIS PAGE	19. SECURITY CLASSIFICATION OF ABSTRACT	20. LIMITATION OF ABSTRACT
Unclassified	Unclassified		